Clays and Clay Minerals, Vol. 49, No. 3, 189–196, 2001.

MICA STRUCTURE AND FIBROUS GROWTH OF ILLITE

NECIP GÜVEN

Department of Geosciences, Texas Tech University, Box 41053,
Lubbock, Texas 79409, USA

Abstract—The relative growth rates of the three joint chains of silica tetrahedra and metal octahedra in the [100], [$\bar{1}$10] and [$\bar{1}\bar{1}$0] directions within the mica layer (referring to the 1*M* unit-cell) seem to control the morphology of mica crystallites. Laths and fibers are the products of relatively fast growth along the [100] direction compared to growth along the [$\bar{1}$10] and [$\bar{1}\bar{1}$0] directions. The (010) growth front in 1*M* micas with *trans*-octahedral vacancies exposes a pair of reactive OH ions that can form organic or inorganic complexes and 'poison' the growth on the (010) face.

Authigenic illite fibers in two sandstones with contrasting lithologies are found to have grown on mica or kaolinite cores. Illite fibers appear in single sets or in multiple sets, 120° apart. This texture seems to be related to the stacking sequence of the layers in mica or kaolinite in the core of these fibers.

Key Words—Illite Fibers, Illite Laths, Mica Structure.

INTRODUCTION

Authigenic illites precipitated from formation waters in sandstone pores appear frequently in the form of laths and fibers. This fibrous illite may severely affect the porosity and permeability of reservoir sandstones and cause serious problems for hydrocarbon production. Diagenetic growth of fibrous illite in sandstone reservoirs was first documented by Wilson and Pittman (1977). Since then fibrous illite in sandstones has been the subject of a large volume of literature. However, how and why fibrous illites form are not yet understood. This report addresses the question of how a mineral with a dioctahedral mica structure can grow as fibers. The crystal structural factors favoring the fibrous growth of illite are discussed by considering two sets of data: (1) the morphology and texture of fibrous illites in two sandstones with contrasting mineralogy, depositional environment and fabric; and (2) the results of attempts to grow fibrous illites in the laboratory.

MORPHOLOGICAL AND TEXTURAL FEATURES OF FIBROUS ILLITES IN TWO SANDSTONES WITH CONTRASTING MINERALOGY AND FABRIC

Two sandstones were studied with a JEM-100CX Analytical Electron microscope operated at 100 keV potential and 100 μA electron beam current. Carbon-platinum-coated sandstone chips were first examined with scanning electron microscopy (SEM). Suspensions of clay particles and their aggregates were extracted by sedimentation in distilled and deionized water containing traces of tertiary butylamine to reduce surface tension. A drop from each of these suspensions was dried on a Cu grid covered with a Formvar film and subsequently coated with C/Pt. The morphological features of the clay particles were then studied with transmission electron microscopy (TEM) and scanning transmission electron microscopy (STEM). Energy-dispersive analyses of X-ray spectra (EDAX) obtained from the illite particles were performed to determine the chemistry of the individual clay particles. Characteristic X-ray spectra from the individual clay particles were obtained using a KEVEX microanalyzer. The latter was equipped with a Si(Li) solid-state detector with ultra-thin window providing a resolution of 155 eV. A selected area of ~0.5 μm^2 of a clay particle was scanned in STEM mode for up to 200 s at 100 keV potential to minimize K migration under the 100 μA electron flux. The energies of the characteristic X-ray photons were then processed by a multichannel analyzer with an on-line computer using KEVEX's TEMSTAR software. The net spectral intensities were calculated after corrections for background and escape peaks. These spectral intensities were then converted to atomic ratios by the thin-film approximation (Goldstein, 1979) using Si as the reference element:

$$N_X/N_{Si} = k_{(X-Si)}(I_X/I_{Si})$$

where N_X/N_{Si} is the atomic ratio of element X to Si and I_X/I_{Si} is their spectral intensity ratio. The proportionality constants $k_{(X/Si)}$ were obtained from the thin mica flakes with known chemical compositions under the same conditions: $k_{(Al/Si)}$ = 1.156 (from muscovite); $k_{(K/Si)}$ = 0.888 (from muscovite); $k_{(Mg/Si)}$ = 1.386 (from phlogopite); and $k_{(Fe/Si)}$ = 0.733 (from annite).

Because of its low energy, X-ray spectra from oxygen are not used for quantitative analysis. Furthermore, because of the overlapping spectral lines of NaKα (1.041 keV) and CuLα (0.928 keV), weak Na lines are not included in the analysis. The results are described below.

Fibrous illites in St Peter Sandstone

St Peter Sandstone is a well known shallow-marine Ordovician formation extending over three states from

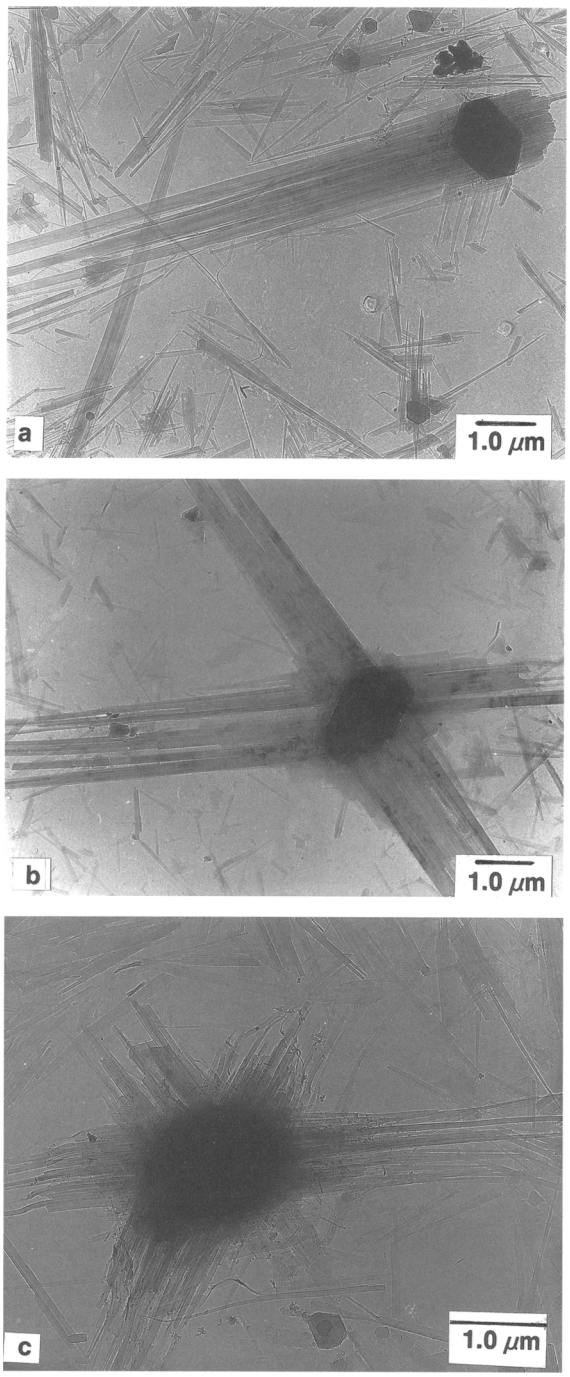

Figure 1. Sets of illite laths and the euhedral kaolinite core in St Peter Sandstone: (a) single set of laths; (b) double set of laths 120° apart; and (c) triple set of laths 120° apart.

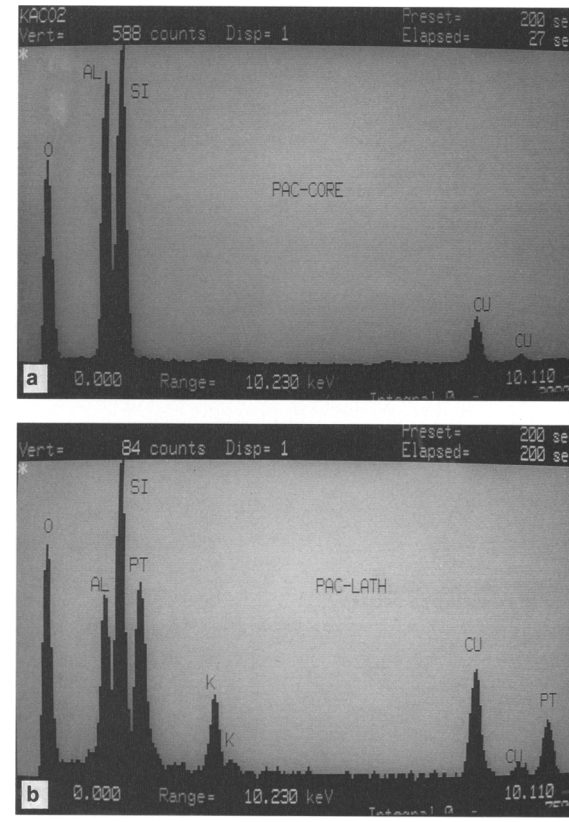

Figure 2. X-ray spectra obtained from (a) the kaolinite core in Figure 1a, and (b) from the single set of illite laths in the same figure. The Cu and Pt lines belong to the sample holder and coating metal.

Kansas through Missouri to Illinois (Thompson, 1991). The samples were obtained from the Pacific Glass Sand Quarry, which is located about a half mile east of Pacific in St Louis County, Missouri. The sandstone in this location is subaerially exposed and consists of extremely clean, well sorted and well rounded polycyclic quartz grains that comprise >99% of the rock. The sandstone in this locality is very friable and lightly cemented. It is highly porous and permeable and therefore allows infiltration of leachates from the soil above. The total amount of the fine material (<200 μm) was determined to be ~0.31% (Koenig, 1961).

Illite and kaolinite appear as an impurity below the 0.5% level. Illite fibers in the St Peter Sandstone appear to have grown from the edges of a kaolinite (Figure 1). The illite fibers range in length from 1 to 10 μm and appear in sets of parallel fibers growing from a euhedral kaolinite platelet. Single, double and triple sets of illite fibers, 120° apart, are rather common as illustrated in Figure 1. Euhedral platelets of the kaolinite core range from 1.0 to 2.0 μm across. X-ray spectra in Figures 2a and 2b were obtained from the core kaolinite and from the single set of fibers. The spectra clearly establish the identities of the core as kaolinite and the fibrous overgrowth as illite. These core kaolinites must have precipitated before the overgrowth of illite fibers on them. Kaolinite was probably the early weathering product of K-feldspar impurities

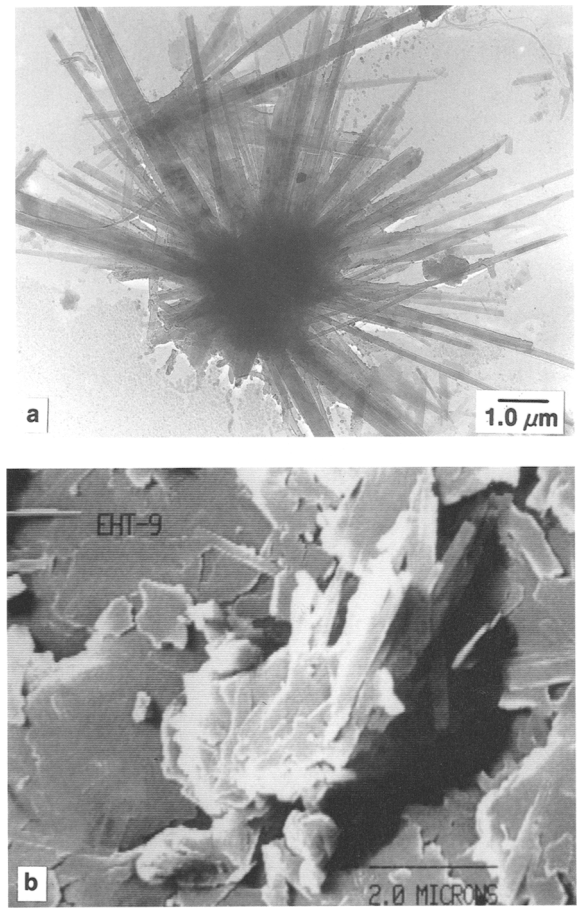

Figure 3. Radial growth of authigenic illite laths in Rhourde El Baguel sandstone from Eastern Sahara: (a) TEM image, and (b) SEM image of another illite aggregate.

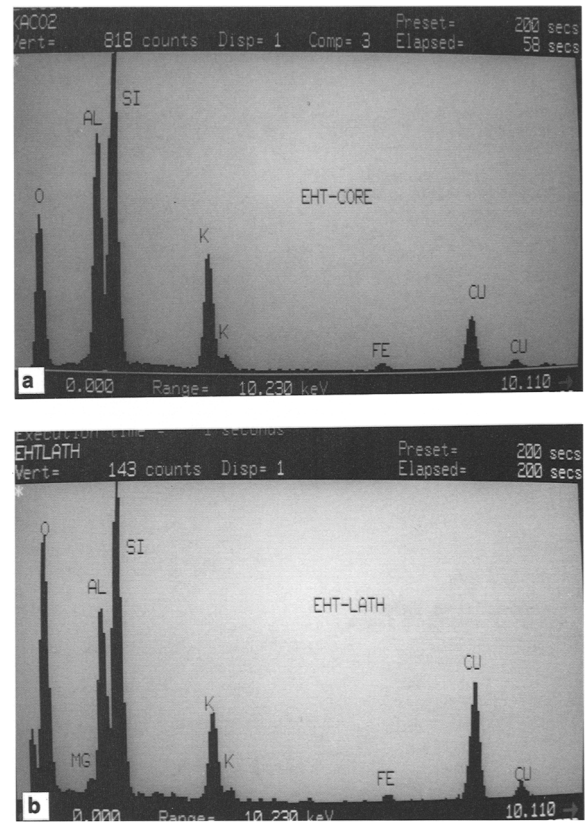

Figure 4. X-ray spectra obtained from the (a) dense core of the aggregate in Figure 3a, and (b) illite laths in the same figure.

subjected to the infiltrating leachates from the overlying soil.

Fibrous illites in Rhourde El Baguel Sandstone, Eastern Sahara

The sandstone is from the giant oil field in Rhourde el Baguel in Eastern Sahara and is Cambro-Ordovician in age. This sandstone was described by Triplehorn (1967) and recently re-examined by Steve Franks (pers. comm.). Their findings are summarized below. The sandstone is non-marine, poorly sorted, micaceous and feldspathic. It is cemented extensively and contains ~75% quartz, 20% fibrous illite and a few percent of unaltered feldspars and muscovite. Fibrous illite fills the pores as the main cementing agent and was a diagenetic alteration product of K-feldspar and mica. Fluid flow rate in such a pore system filled with clays is expected to be much lower than in the highly porous St Peter Sandstone. The current burial depth of the sandstone is estimated to be 1500 m. Oxygen isotopic composition as determined by Franks confirms the formation of illite by the alteration of the detrital feldspars, mica and clays in non-marine formation waters.

The TEM images in Figure 3 illustrate the common morphology and texture of fibrous illites in the reservoir sandstone from Rhourde El Baguel, Eastern Sahara. The illite laths range in length from 0.3 to 30 μm and show a radial growth from a dense core in bundles. In some of these illite clusters there is an apparent preference for the sets of these laths in two or three directions, 120° apart. Common clusters of illite fibers show no apparent preferred orientations as illustrated in Figure 3a. The SEM image in Figure 3b reveals that the illite fibers not only grow at the edges of a core mica but also epitaxially on it. Characteristic X-ray spectra were collected from the laths and their dense cores (Figures 4a, 4b). Tables 1 and 2 list the chemical compositions (atomic ratios) of the cores and laths that were calculated from the X-ray spectra. The chemical formulae below are derived from these data on the basis of the anionic framework of $O_{10}(OH)_2$:

core: $K_{0.91}(Al_{0.77}Si_{3.23})(Al_{1.73}Mg_{0.24}Fe_{0.07})O_{10}(OH)_2$

laths: $K_{0.86}(Al_{0.73}Si_{3.27})\ (Al_{1.71}Mg_{0.31}Fe_{0.04})O_{10}(OH)_2$

The chemical data indicate that the variations in Si, Al

Table 1. Atomic ratios of elements derived from the X-ray spectral intensities obtained from the cores of illite aggregates.

	Mg	Al	K	Fe	Si
	0.092	0.758	0.273	0.010	1.00
	0.056	0.839	0.355	0.018	1.00
	0.093	0.753	0.271	0.010	1.00
	0.067	0.780	0.289	0.019	1.00
	0.072	0.804	0.294	0.015	1.00
	0.072	0.802	0.304	0.019	1.00
	0.072	0.833	0.286	0.013	1.00
	0.069	0.728	0.258	0.053	1.00
	0.068	0.726	0.259	0.034	1.00
	0.065	0.702	0.244	0.032	1.00
Average:	0.073	0.773	0.283	0.022	1.00

Table 2. Atomic ratios of elements derived from the X-ray spectral intensities obtained from individual laths.

	Mg	Al	K	Fe	Si
	0.093	0.682	0.250	0.020	1.00
	0.096	0.715	0.274	0.014	1.00
	0.111	0.656	0.263	0.024	1.00
	0.082	0.759	0.259	0.019	1.00
	0.110	0.742	0.248	0.010	1.00
	0.089	0.740	0.257	0.010	1.00
	0.111	0.700	0.242	0.010	1.00
	0.092	0.757	0.253	0.012	1.00
	0.089	0.763	0.276	0.020	1.00
	0.083	0.760	0.266	0.010	1.00
	0.105	0.758	0.248	0.012	1.00
	0.100	0.769	0.251	0.012	1.00
	0.087	0.759	0.254	0.013	1.00
	0.102	0.769	0.286	0.013	1.00
	0.087	0.787	0.299	0.014	1.00
	0.073	0.785	0.264	0.011	1.00
	0.073	0.800	0.286	0.015	1.00
Average:	0.094	0.747	0.263	0.014	1.00

and Fe between the cores and laths are within the standard errors of measurement. The only significant differences in the chemistries of the laths and cores are related to the relative deficiency of K and maybe a slight excess of Mg in the laths. The difference in K can be explained by the long edge faces (010) along which K ions can be readily released. The laths are elongated along the *a* axis referring to the 1*M* mica unit-cell and they sometimes display perfect endings consisting of (110) and (1$\bar{1}$0) faces.

EXPERIMENTAL RESULTS FROM THE SYNTHESIS OF FIBROUS ILLITE

The first attempt to synthesize fibrous illite was made by Güven *et al.* (1982) to understand the reaction kinetics favoring fibrous growth. For this purpose, fine albite powders were subjected to a hydrothermal alteration with KCl solutions at 200°C/500 bar for 24–84 d. Negligibly small quantities of fibrous illite were found as accessories to large amounts of lamellar (platy) illites under neutral pH conditions. Later, Champion (1989) synthesized both laths and lamellar illites using K-Si-Al gels under hydrothermal conditions at 300–350°C and 12 kbar for 14–32 d. The effects of octahedral substitutions of Mg^{2+} or Fe^{3+} for Al on illite morphology were studied by Güven and Huang (1991). For this purpose, first the glasses were made from gels with the appropriate chemical composition and then these glasses were subjected to hydrothermal alterations at 300°C and 500 bar for 35–90 d. These experiments yielded large amounts of illite-smectite mixed layers (I-S) in the form of foliated flakes and compact lamellar (platy) aggregates. Laths were found only in the systems with no Mg^{2+} or Fe^{3+} substitutions but in negligibly small amounts.

Large quantities of fibrous illite, remarkably similar to those in reservoir sandstones, were synthesized for the first time by Small *et al.* (1992), Small and Manning (1993) and Small (1993). These investigators per-

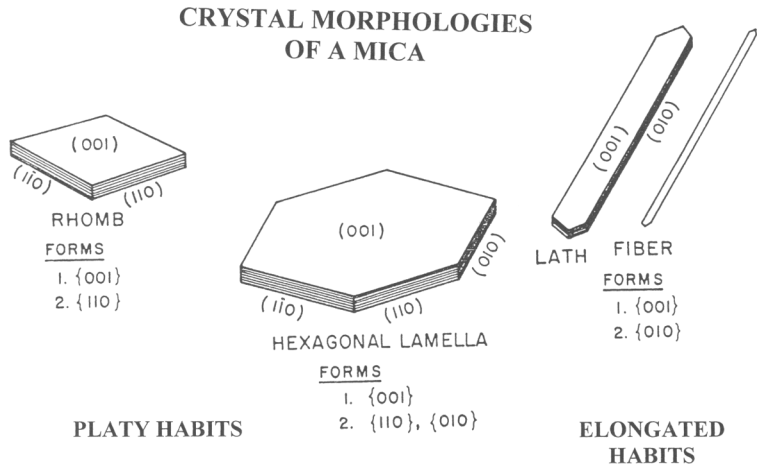

Figure 5. Variations in the idiomorphic forms of a mica and their prominent faces: basal faces (001) and prismatic faces (010), (110) and (1$\bar{1}$0).

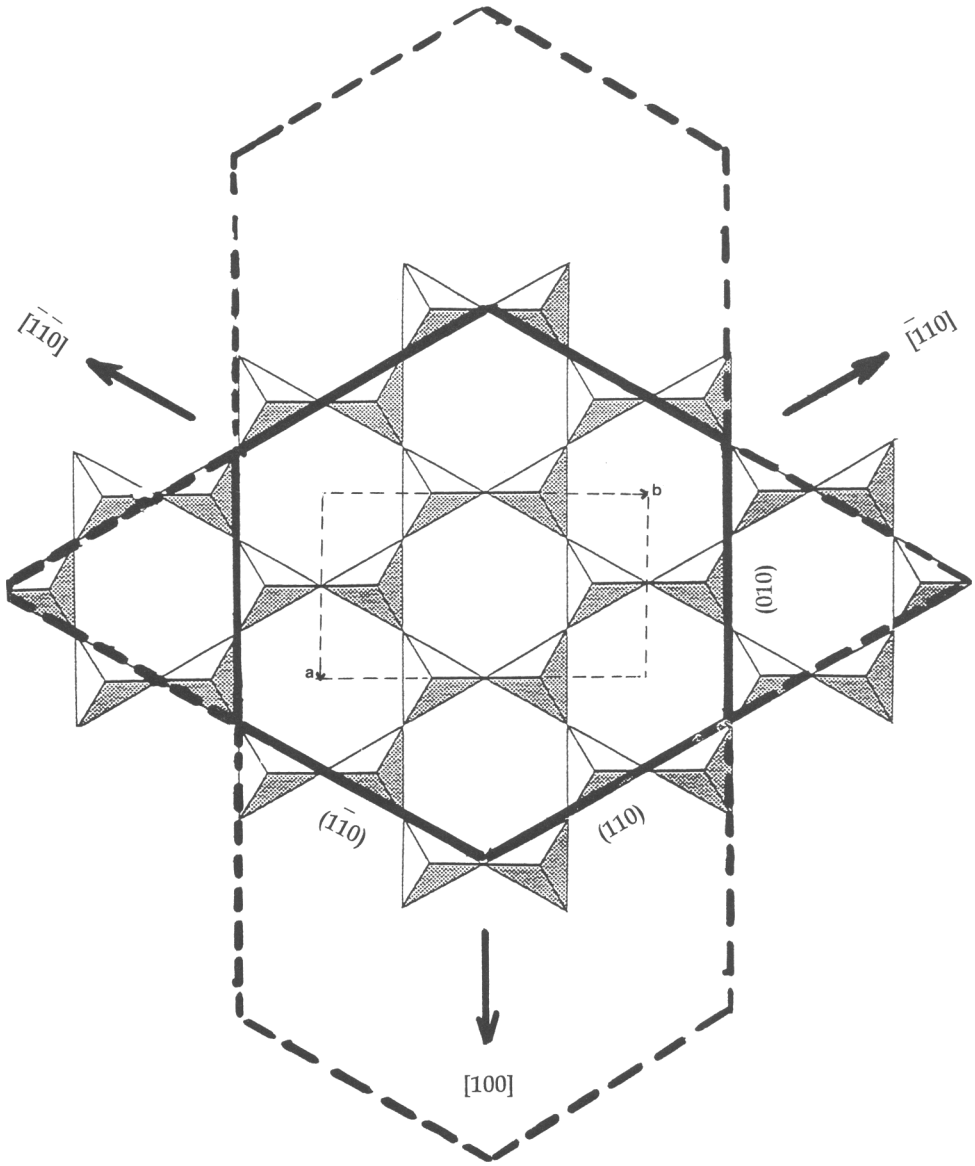

Figure 6. Mica structure (only one sheet of the silica tetrahedra shown) and the relationships between its crystal habits.

formed an experimental diagenesis of illite on sand grains at 150–350°C and 750–1000 bar for periods of up to 71 d. The precipitation of large amounts of illite fibers was found in oxalate-bearing solutions. Most recently, Bauer *et al.* (2000) were able to synthesize both platy and lath-shaped illites in the absence of organic acids at temperatures of 35 to 80°C over a long period of time up to 4 y. They conducted the experiments using kaolinite and KOH as reactants and found that the laths are transient and eventually recrystallize to platy illites. Laths were found to appear at lower levels of supersaturation and at a relatively lower growth rate than the platy illites. Earlier, in a rather comprehensive review of illite diagenesis in sandstones, Lanson and Champion (1991) and Lanson *et al.* (1996) had reached a similar conclusion that the illite laths are metastable forms that eventually recrystallize to platy forms, which is the ideal crystal form expected from a layer silicate.

MICA STRUCTURE AND GROWTH OF ILLITE FIBERS

The crystallographic features of fibrous illites were described by Güven *et al.* (1980). They pointed out that illite laths have a dioctahedral 1*M* mica structure with *trans*-octahedral vacancies and the laths are parallel to the *a* crystallographic axis. Figure 5 shows possible variations in the crystal habit of a mica with the prominent

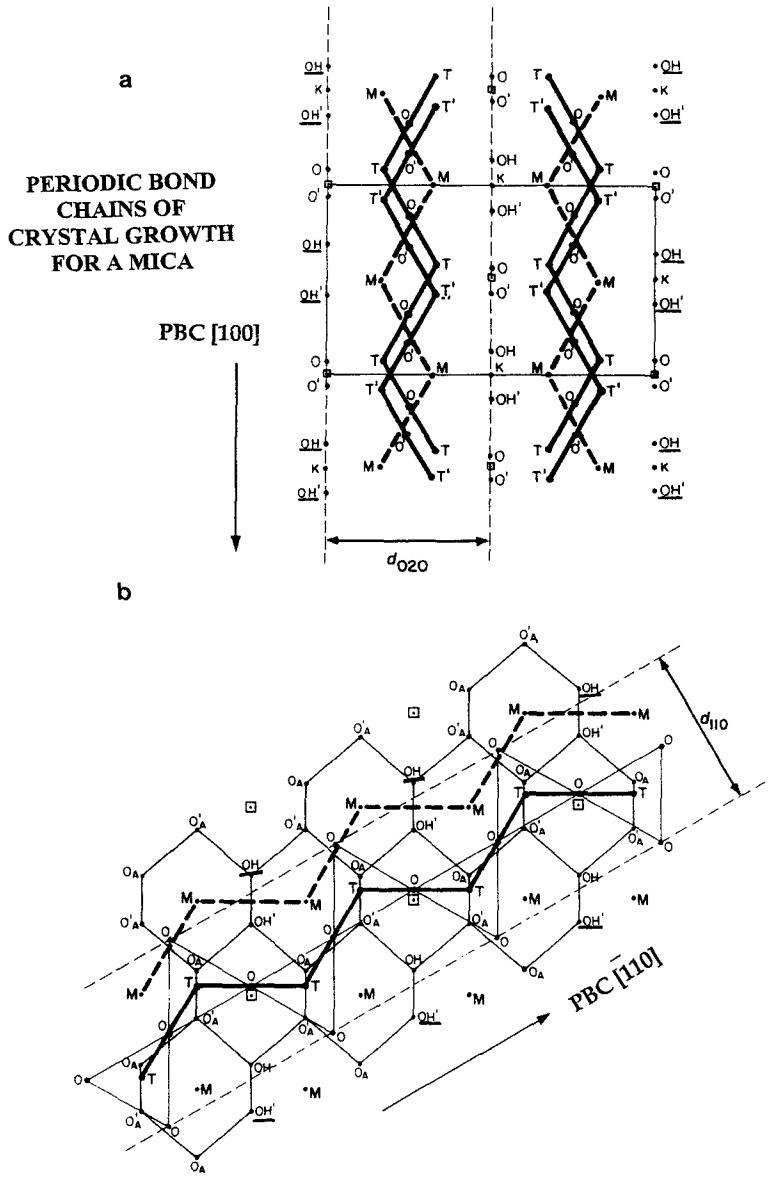

Figure 7. Projections of the periodic bond chains (PBC) in a 1*M* mica structure along the [001] direction: (a) atomic configuration of the [100] chain exposing OH, K and octahedral *trans* vacancies on the (010) faces of laths; and (b) [$\bar{1}$10] bond chains and the configuration of the ions and octahedral *cis* sites exposed on the (110) faces. Primed letters such as O′, OH′ and T′ represent the atomic positions below the octahedral cations and □ octahedral vacancies.

basal and prismatic faces on these forms. Elongated habits of illites display aspect ratios (length/width) ranging from 3 to 50 or more. The laths with aspect ratios >50 appear like fibers, especially in low-magnification images. Depending on their thicknesses, the laths and fibers can be rigid or flexible. Flexible laths are often referred to as ribbons; flexible fibers are referred to as filaments, whiskers or hairs. Figure 6 illustrates the intimate relationships between the different mica habits and the silica chains in the mica structure. Chains of metal octahedra (Figure 7) sharing oxygen ions with silica tetrahedra have the same relationships as the silica chains with the mica habits.

The crystal structure of a 1*M* mica provides a reasonable explanation for its prominent platy morphology. There are three prominent growth directions, namely [100], [$\bar{1}$10] and [$\bar{1}\bar{1}$0] within a mica layer (Figure 6). There is no growth chain exposed in the [001] direction; the growth of a mica in the [001] direction requires two-dimensional nucleation or screw dislocations. However, the building blocks of a mica (silica tetrahedra and metal octahedra) can be readily

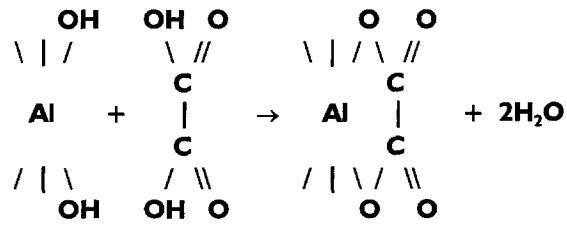

Figure 8. Possible reaction mechanism between oxalic acid and the hydroxyls exposed on the (010) growth front of illite lath.

attached to the growth chains along the [100], [$\bar{1}$10] and [1$\bar{1}$0] directions without a need for nucleation. These growth chains are often referred to as "periodic bond chains" (Hartman, 1972) and consist of silico-metal copolymers in micas (Figure 7). They are 120° apart in the mica structure and provide equally favorable attachment sites for the lateral growth of a mica layer. The growth fronts (010), (110) and (1$\bar{1}$0) marked in Figure 6 are parallel to the growth chains [100], [$\bar{1}$10] and [$\bar{1}\bar{1}$0], respectively.

Three different crystal habits of a mica (Figure 5) may develop, depending on the growth rates on the (010), (110) and (1$\bar{1}$0) fronts: (1) a hexagonal habit (which is actually pseudo-hexagonal due to monoclinicity of the layer) develops when the growth rates are equal on all of the three growth fronts above; (2) rhombs (actually pseudo rhombs) may form when the growth rate on the (010) front is faster than on the (110) and (1$\bar{1}$0) fronts; and (3) laths and fibers develop when the growth rate on the (010) front is slower than on the (110) and (1$\bar{1}$0) fronts.

The growth of the illite laths and fibers must therefore be related to some reaction retarding the growth rate on the (010) front. The atomic configurations exposed on the (010), (110) and (1$\bar{1}$0) fronts are rather different. The (010) front exposes pairs of octahedral OH ligands (Figure 7a) that can readily form complexes with organic or inorganic functional groups. Organic acids in the formation waters can develop complexes with the OH pairs and stop the further growth of the (010) front. The (110) and (1$\bar{1}$0) growth fronts are rather rough with many kinks; they expose octahedral *cis*-sites occupied by Al and numerous broken bonds. The (110) and (1$\bar{1}$0) fronts may, therefore, grow faster than the (010) front.

Experimental studies on illite diagenesis by Small *et al.* (1992), Small and Manning (1993) and Small (1993) demonstrated the precipitation of large quantities of fibrous illite on sand grains from solutions containing oxalate anions. The importance of organic acids, especially carboxylic acids, in sandstone diagenesis was well documented by Surdam *et al.* (1984, 1989). They reported that these organic acids are rather common and may reach 5000 ppm or more in the formation waters of clastic reservoirs. For instance, difunctional oxalic acid can form complexes with the pairs of hydroxyl ligands exposed on the (010) growth fronts according to the reaction indicated in Figure 8.

The Al oxalate complex on the (010) growth front may then stop the growth until the decay of the oxalate anion. It is possible that there may be similar reactions with other organic and inorganic functional groups leading to the 'poisoning' of the (010) front; this appears to be the key for the development of illite fibers.

The texture of fibers with a preferred arrangement of illite fibers in well defined sets seems to be related to the stacking sequences of the layers in the crystal structure of the core mica or kaolinite in the sandstones examined in this study. The 1*M* mica or 1*Tc* kaolinite core will have no rotations between their layers but they may have stacking faults involving 120° rotations resulting in twinning. It will then be possible to relate a single set of illite fibers with a 1*M* mica or 1*Tc* kaolinite core. Double and triple sets of illite fibers 120° apart can then grow from these cores with stacking faults. An extensively altered mica with disturbed stacking sequences, like the micas in the East Saharan sandstone, may then serve as a core where illite fibers can grow radially in several irrational directions. Thus, the stacking sequence of the layers in the core mica or kaolinite seems to have a reasonable influence on the texture, *i.e.* the arrangement of illite fibers growing from it.

REFERENCES

Bauer, A., Velde, B. and Gaupp, R. (2000) Experimental constraints on illite crystal morphology. *Clay Minerals,* **35,** 587–597.

Champion, D. (1989) Etude des mechanisms de transformation des interstratifies illite/smectite au cours de la diagenese. Ph.D. thesis, University Paris XI-Orsay, France, 204 p.

Goldstein, J.I. (1979) Principles of thin film X-ray microanalysis. Pp. 83–120 in: *Introduction to Analytical Electron Microscopy* (J.T. Hren, J.I. Goldstein and D.C. Joy, editors). Plenum Press, New York and London.

Güven, N. and Huang, W.L. (1991) Effects of octahedral Mg^{2+} and Fe^{3+} substitutions on hydrothermal illitization reactions. *Clays and Clay Minerals,* **39,** 387–399.

Güven, N., Hower, W.F. and Davies, D.K. (1980) Nature of authigenic illites in sandstone reservoirs. *Journal of Sedimentary Petrology,* **50,** 761–766.

Güven, N., Lafon, G.M. and Lee, L.J. (1982) Experimental hydrothermal alteration of albite to clays: preliminary results. *Proceedings of the International Clay Conference 1981.* Elsevier Scientific Publishing Company, pp. 495–512.

Hartman, P. (1972) Structure and morphology. Pp. 367–402 in: *Crystal Growth—An introduction.* North-Holland Publisher, Amsterdam.

Koenig, J.W. (1961) *The Stratigraphic Succession in Missouri.* State of Missouri, Department of Business Administration, pp. 13–31.

Lanson, B. and Champion, D. (1991) The I/S to illite reaction in the late stage diagenesis. *American Journal of Science,* **291,** 473–506.

Lanson, B., Beaufort, D., Berger, G., Baradat, J., and Lacharpagne, J.C. (1996) Illitization of diagenetic kaolinite-to-dickite conversion series: late-stage diagenesis of the

lower Permian Rotliegend Sandstone reservoir, offshore of the Netherlands. *Journal of Sedimentary Research,* **66,** 501–518.

Small, J.S. (1993) Experimental determination of the rates of precipitation of authigenic illite and kaolinite in the presence of aqueous oxalate and comparison to the K/Ar ages of authigenic illite in reservoir sandstones. *Clays and Clay Minerals,* **41,** 191–208.

Small, J.S. and Manning, D.A.C. (1993) Laboratory reproduction of morphological variation in petroleum reservoir clays: Monitoring of fluid composition during illite precipitation. Pp. 181–212 in: *Geochemistry of Clay Pore Fluid Interactions* (D.A.C. Manning, P.L. Hall and C.R. Hughes, editors). Mineralogical Society/Chapman & Hall, London.

Small, J.S., Hamilton, D.L. and Habesh, S. (1992) Experimental simulation of clay precipitation in reservoir sandstones 2: Mechanism of illite formation and controls on morphology. *Journal of Sedimentary Petrology,* **62,** 520–529.

Surdam, R.C., Boese, S.W. and Crossey, L.J. (1984) The chemistry of secondary porosity. Pp. 127–149 in: *Clastic Diagenesis* (D.A. MacDonald and R.C. Surdam, editors). American Association of Petroleum Geologists, Tulsa, Oklahoma.

Surdam, R.C., Crossey, L.J., Hagen, E.S. and Heasler, H.P. (1989) Organic-inorganic interactions and sandstone diagenesis. *AAPG Bulletin,* **73,** 1–23.

Thompson, T.L. (1991) *Paleozoic Succession in Missouri Part 2. Ordovician System.* Report of Investigations No. 70, Missouri Department of Natural Resources, pp. 69–78.

Triplehorn, D.M. (1967) Occurrence of pure well-crystallized 1M illite in Cambro-Ordovician sandstone from Rhourde El Baguel field, Algeria. *Journal of Sedimentary Petrology,* **37,** 879–884.

Wilson, M.D. and Pittmann, E.D. (1977) Authigenic clays in sandstones: Recognition and influence on reservoir properties and paleoenvironmental analysis. *Journal of Sedimentary Petrology,* **47,** 3–31.

E-mail of corresponding author: necip.guven@ttu.edu

(Received 17 August 2000; revised 14 December 2000; Ms. 482; A.E. Stephen Altaner)